Service Guarantee in Multi-Priority Traffic: A Spatial Network Calculus Perspective

Xiaohang Zhou*, Yi Zhong*, *Senior Member, IEEE*, Ke Feng†, Donglin Jia*
*School of Electron. Inf. & Commun., Huazhong University of Science and Technology, Wuhan, China
†INRIA-ENS, Paris, France

***Abstract*—This paper extends classical network calculus to spatial scenarios, adapting it to manage the spatial distribution of links in wireless device-to-device networks. Considering the wireless network with multi-priority users, we propose two regulations to characterize the upper bounds of the total power for transmitters and total received interference for users. Using the bipolar model, we introduce a power resource allocation strategy tailored for multi-priority traffic. Inspired by Shannon's theorem, we define a logarithmic relationship between the required signal-to-interference-plus-noise ratio (SINR) and transmitter power for different user classes. This method aims to ensure quality of service (QoS) of all links across varying traffic priorities by integrating spatial and power allocation regulations. The result is enhanced network performance, quantified by improvements in link reliability and the establishment of lower bounds on SINR thresholds.**

***Index Terms*—Network Calculus, performance guarantees, stochastic geometry, point process, wireless network.**

I. Introduction

A. Motivations

The expansion of the Internet has significantly diversified network services, elevating user expectations for quality of service (QoS). Meanwhile, users engaged with various services exhibit diverse requirements from the network, which necessitates not only addressing the demands of users with higher needs but also considering the service experience of those with lesser requirements. Although the next generation of advanced mobile communication systems, 6G, continues to push forward research in energy efficiency, ultra-reliable and low-latency, providing service guarantee for all users in any large-scale multi-priority wireless network remains a challenging yet critical endeavor [1], [2]. Hence, accommodating the varied signal-to-interference-plus-noise ratio (SINR) requirements of different user classes are the principal focus of this paper.

In response to the diverse demands of users, it is imperative to implement precise power allocation strategy tailored to each user class or traffic priority. Network calculus is dedicated to assessing worst-case performance, proving deterministic bounds on delay, backlog and other QoS parameters in wireline networks. In contrast, wireless networks can utilize stochastic geometry to regulate the spatial distribution of network nodes and derive provable performance guarantees. Given the varying priorities of network traffic and the scarcity of network resources, effective regulation of spatial network deployment and strategic allocation of limited wireless resources are essential to meet these multi-priority traffic demands.

B. Related Works

In scenarios where resource availability is constrained, the allocation of priority becomes a pivotal consideration. Choi et al. [3] suggest a mechanism where vehicles engage in transmission based on possessing the highest priority among their neighboring vehicles. Kumar and colleagues [4] introduce a method for assigning terminal priorities, factoring in both the ongoing service and the terminal's location. Abdel-Hadi [5] focuses on finding the optimal solution for the resource allocation problem that includes users with priorities. Lee's work [6] delves into the realm of optimal power allocation, prioritizing services and thereby directing power allocation in alignment with these priorities. In [4]–[6], the authors focused on the multi-priority mechanisms and power resource allocation strategies in communication networks, which improves performance and fairness to terminal users. However, the link performance of all priorities may not be deterministically guaranteed due to the uncontrollable randomness of the transmitter locations. Thus, in order to resolve this issue, the spatially regulated point process should be considered.

Employing an appropriate point process is critical for accurately modeling the spatial distribution of nodes in wireless networks. Zhong [7] considers the commonly used Poisson bipolar model to depict the spatial distribution of the devices, characterizing the massive properties of massive and sporadic access. When transmitters are modeled as a Poisson point process and implemented an access control protocol like CSMA, the effective transmitters are modeled as a Matérn hardcore point process [8]. In [9], an extension of Matérn hardcore point process is used, where the competition is based on pair-wise SIR protection zones with the modification to the RTS/CTS mechanism which defines a receiver-centered protection zone to restricts other transmitters' activity within the area. Mishra et al. [10] employ stochastic geometry to realistically model automotive radar interference, incorporating the Matérn point process to account for the spatial mutual exclusion of vehicles. Di Renzo et al. [11] uses Matérn hardcore point process for modeling base stations within cellular networks. Chen [12]

This research was supported by the National Natural Science Foundation of China (NSFC) grant No. 62071190 and No. 62471193, and the National Key Research and Development Program of China (2020YFB1807700).

The corresponding author is Yi Zhong (yzhong@hust.edu.cn).

analyzes the stable packet arrival rate region in discrete-time slotted random access network by arranging transmitters as Matérn hardcore point process.

Performance guarantees in wireless networks encompass link reliability, rate and latency guarantees for all links. Miao [13] proposes joint power allocation algorithm with QoS guarantee using convex optimization method which satisfies the minimum rate constraint of delay-constraint service and proportional fairness of best-effort service. Liu's research [14] proposes an algorithm that not only enhances the utility for best-effort users but also diminishes the outage probability for rate-constrained users.

In this study, we adapt the classical network calculus framework [15]–[17] to regulate the distribution of transmit-receive pairs in wireless device-to-device networks. The seminal work of Cruz in classical network calculus introduces the (σ, ρ) traffic regulation, where σ represents an allowable level of initial burstiness, and ρ sets the upper limit for the long-term average rate. The traffic flow is thus bounded by a baseline constant σ and an additional rate ρ does scale the length of the time interval [17].

Expanding these principles into spatial contexts, [18] applies the parameters σ, ρ, and an additional parameter ν to govern the number of wireless links, the cumulative received power, and the interference within large-scale wireless networks. This methodology leads to the development of (σ, ρ, ν)-ball regulation and (σ, ρ, ν)-shot-noise regulation in spatial network calculus. These regulations are extended to provide a theoretical framework to ensure service guarantees for multi-priority traffic demands in our study. Furthermore, our research proposes a unique power resource allocation strategy. This strategy is specifically designed to manage the allocation of power in a bipolar network architecture [19], where the distribution of transmitters follows a hardcore process, and takes into account the presence of users or traffic of varying priorities.

C. Contributions

Our approach innovatively expands traditional network calculus into spatial domains, integrating it with advanced power allocation strategies to effectively manage diverse network demands. This integration of ball regulation and shot-noise regulation with innovative power allocation is key in maintaining service quality within a bipolar model, essential in multi-priority traffic environments. Our research contributions are summarized as follows:

- We extend spatial network calculus and performance guarantees to wireless device-to-device networks with multi-priority traffic and users.
- We propose a power allocation strategy that optimally distributes limited power resources based on user priorities.
- By combining ball and shot-noise regulation with our power allocation strategy, we derive lower bounds for link reliability and establish robust conditions to ensure quality of service across various network scenarios.

This paper is organized as follows: Section II elaborates on the system model considered in this paper. In Section III, we propose several spatial regulations and power allocation strategy to regulate the wireless network configuration. In Section IV, we derive the link reliability lower bound for the whole wireless network based on the regulations and strategy. Numerical results are provided in Section V, and finally, the conclusion is summarized in Section VI.

II. System Model

This paper considers all links in large-scale wireless networks with multi-priority traffic. The Poisson point process (PPP) model assumes that all nodes are independent and ignores the effect of spatial mutual exclusion. To guarantee the quality of service for multi-priority users and provide more realistic interference effects, the Matérn hardcore point process (MHCPP) is used instead of PPP (see Fig. 1). The MHCPP model introduces mutually exclusive regulation to the deployment of transmitters in wireless networks. This ensures that the distance between transmitters is not less than the hardcore distance H. We assume that the transmitters are distributed as a MHCPP of type II, which has a higher average density than type I, in order to accommodate more users. Furthermore, the transmitter locations for users with different priorities are modeled as independent hardcore point processes, which are thinned from Poisson point processes with varying hardcore distances. And we consider that the retained links in the network are always active to derive the worst-case bounds, without considering the impact of queuing.

Assume that there are M classes of users in a large wireless network with different target SINR thresholds, $\theta_1, \theta_2, \ldots, \theta_M$, respectively, and assume that $\theta_1 > \theta_2 > \ldots > \theta_M > 0$. We use a stationary and ergodic point process Φ_i on $\mathbb{R}^2$ to denote the MHCPP which models the transmitter locations corresponding to the i-th user class, and the hardcore distance is H_i. We define $\Phi \triangleq \bigcup\{\Phi_i\}$ as the superposition of the point processes corresponding to different classes of users. Note that the point process Φ_i is independent of each other. Use Ψ_i to denote the point process corresponding to the receiver locations which is jointly stationary and ergodic with Φ_i. The link distance $r_0 > 0$ between the receiver and its dedicated transmitter is fixed in our assumption, such as some direct communications. In order to meet requirements for different user classes, we consider a power control scheme which assigns different power P_i to their corresponding transmitters for the i-th user class. Without loss of generality, we assume that the bandwidth is normalized to 1.

In our study, we hypothesize that the channels within small-scale wireless network models are characterized by two cases, i.e. Rayleigh fading and remain without fading. Using the bounded, non-increasing, continuous and integrable function $\ell(r)$ as the path loss function and r_0 denoting the distance from the receiver to its dedicated transmitter, we can obtain the representation of SINR for the i-th user class as

$$\mathrm{SINR}_i = \frac{P_i h_x \ell(r_0)}{I + W}, \tag{1}$$

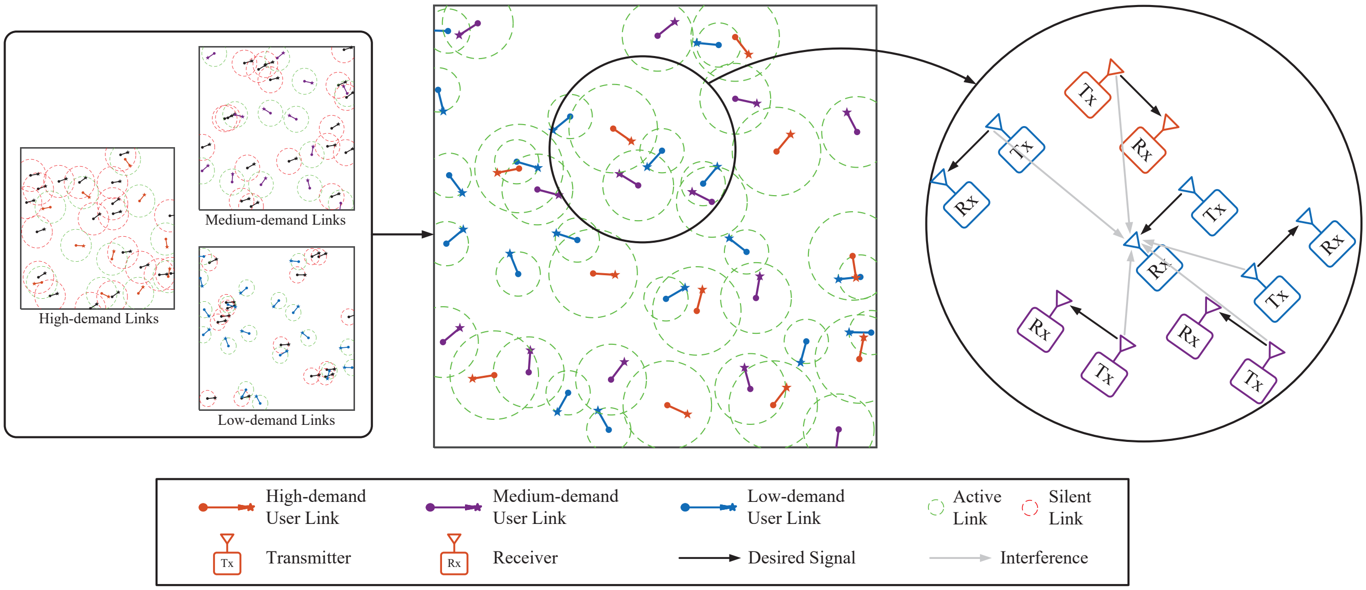

Fig. 1. Diagram of a bipolar network. Solid dots within dashed circles represent transmitters, distributed as a PPP with intensity $\lambda = 0.3$. Stars mark the uniformly distributed receiver locations. Transmitters and receivers are separated by a fixed distance $r_0 = 0.5$ meters. The network employs an MHCPP of type II for the different demand links respectively, thinning the PPP where retained transmitters are shown in green dashed circles. Active links are color-coded to indicate user SINR thresholds: orange links represent high threshold users with hardcore distance $H_1 = 1$ meter, purple links represent medium threshold users with $H_2 = 0.8$ meters and blue for low threshold users with $H_3 = 0.5$ meters.

where P_i denotes the transmit power of the transmitter corresponding to the i-th user class, I denotes the interference power of the other signals in the network, from other transmitters in the i-th class and all transmitters in other classes, and W denotes the variance of the additive white Gaussian noise.

We use h_x to denote the small-scale fading from transmitter x to the receiver we are interested in. For the case without fading, we let $h_x = 1$ for all transmitters to obtain a simplified expression for SINR. Assuming that the Rayleigh fading channels are independent and identically distributed (i.i.d.), we have $|h_x| \sim \text{Rayleigh}(1)$ and $|h_x|^2 \sim \text{Exp}(1)$.

III. Spatial Regulations

In point processes without spatial regulations, such as Poisson point processes, obtaining a lower bound for link reliability in wireless networks of arbitrary size is unfeasible due to potential high interference from nearby transmitters. However, by applying spatial regulations, such as thinning a Poisson point process into a hard-core point process, we can establish upper bounds for both total transmitter power and the combined received power plus interference within any area. Introducing spatial exclusion between nodes serves as a spatial regulation, enabling a link reliability lower bound across the network. We will further define power regulation and multi-priority shot-noise regulation and explain their physical significance.

A. Definitions

Let P denote the power of an individual transmitter, which is associated with the SINR threshold θ of the corresponding user. Denote $P_t(r)$ as the total power allocated to transmitters within a circular area of radius r. Based on these notations, we can provide the definitions of (σ, ρ, ν)-power regulation, β-power allocation strategy, and multi-priority $(\sigma_i, \rho_i, \nu_i)$-shot-noise regulation.

Definition 1. *(Strong (σ, ρ, ν)-power regulation). A stationary point process Φ is strongly (σ, ρ, ν)-power regulation if for all $r \geq 0$,*

$$P_t(r) \leq (\sigma + \rho r + \nu r^2)P, \quad \mathbb{P}\text{-}a.s. \tag{2}$$

where P is the power allocated to a single transmitter and σ, ρ, ν are constants.

The strong regulation means that the upper bounds hold within any area of radius r in space. Given the power of a single transmitter for the i-th class of users, an upper bound on the total power of all transmitters corresponding to that class of users in a circle of radius r is

$$P_{ti}(r) \leq (\sigma_i + \rho_i r + \nu_i r^2)P_i, \tag{3}$$

where P_i is the power of a single transmitter related to the i-th user class, $P_{ti}(r)$ denotes the total power of all transmitters corresponding to the i-th user class in a circle of radius r and σ_i, ρ_i, ν_i is related to the hardcore distance of Φ_i.

Lemma 1. *Let H_i be the hardcore distance of the i-th class of users in a network. Any hardcore point process on $\mathbb{R}^2$ with hardcore distance H_i is strongly $\left(1, \frac{2\pi}{\sqrt{12}H_i}, \frac{\pi}{\sqrt{12}H_i^2}\right)$-power regulated [18].*

Proof. Consider the densest packing scenario (see Fig. 2) where $N_i(r)$ represents the total number of transmitters for the

i-th user classes within a region of radius r, and H_i denotes the hardcore distance. Assuming the hardcore condition enforces a minimum distance H_i between any two transmitters, and the theoretical maximum density of a hardcore packing in $\mathbb{R}^2$ is $\frac{\pi}{\sqrt{12}}$, the upper bound of $N_i(r)$ for $r \geq H_i$ is the area of a larger circle of radius $r + H_i$, divided by the area required per transmitter $\pi H_i^2 N_i(r) \leq \frac{\pi^2 (r+H_i)^2}{\sqrt{12}}$. Expanding and rearranging, we have:

$$N_i(r) \leq 1 + \frac{2\pi r}{\sqrt{12} H_i} + \frac{\pi r^2}{\sqrt{12} H_i^2} \tag{4}$$

Hence, we get the conclusion in the Lemma. □

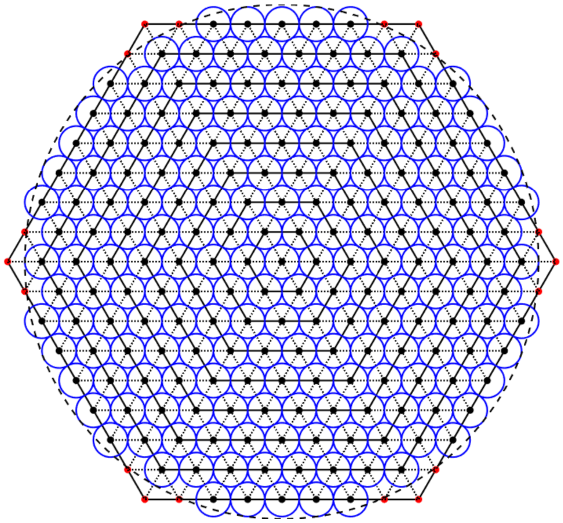

Fig. 2. Diagram of a triangular lattice with eight hexagonal rings of nodes in wireless network. Solid dots represent transmitters, blue circles represent guard zones with a radius of the hardcore distance H, and all retained transmitters are located within a dashed circle with radius r. Ring k contains $6k$ nodes [20].

Definition 2. *(Strong multi-priority $(\sigma_i, \rho_i, \nu_i)$-shot-noise regulation). A stationary point process Φ_i is strongly multi-priority $(\sigma_i, \rho_i, \nu_i)$-shot-noise regulated if, for all non-negative, bounded, and non-increasing functions $\ell : \mathbb{R}^+ \to \mathbb{R}^+$ and for all $R > 0$,*

$$\sum_{x_j \in \Phi_i \cap b(o,R)} \ell(\|x_j\|) \leq \sigma_i \ell(0) + \rho_i \int_0^R \ell(r) \mathrm{d}r + 2\nu_i \int_0^R r\ell(r) \mathrm{d}r, \quad \mathbb{P}\text{-}a.s. \tag{5}$$

When there is only one class of users, i.e., $M = 1$, the multi-priority $(\sigma_i, \rho_i, \nu_i)$-shot-noise regulation simplifies to the standard (σ, ρ, ν)-shot-noise regulation used in spatial network calculus [18].

By considering a special case and setting the function $\ell(\cdot)$ to be identically equal to 1, we derive a formulation akin to the $(\sigma_i, \rho_i, \nu_i)$-ball regulation for all $R > 0$, which can be expressed as:

$$N_i(R) \leq \sigma_i + \rho_i R + \nu_i R^2, \tag{6}$$

where $N_i(R)$ represents the number of transmitters for the i-th class users within a circle of radius R. The $(\sigma_i, \rho_i, \nu_i)$-ball regulation uses the parameters $(\sigma_i, \rho_i, \nu_i)$ to regulate the number of transmitters within a ball centered at the origin with radius R.

Remark 1. *By letting $R \to \infty$, Eq (5) is equivalent to*

$$\sum_{x_j \in \Phi_i} \ell(\|x_j\|) \leq A_{\ell_i}, \quad \mathbb{P}\text{-}a.s., \tag{7}$$

where

$$A_{\ell_i} \triangleq \sigma_i \ell(0) + \rho_i \int_0^\infty \ell(r)\, dr + 2\nu_i \int_0^\infty r\ell(r)\, dr \tag{8}$$

defines the asymptotic upper bound on the total weighted impact of all points in the process, weighted by function ℓ.

The physical meaning of the multi-priority $(\sigma_i, \rho_i, \nu_i)$-shot-noise regulation is that it describes how the power dynamics operate within a spatially distributed network. Specifically, for a user of the i-th class positioned at the origin, this regulation governs the cumulative impact of both useful signal power and interference from other transmitters belonging to the same class as well as from those of other classes. The total impact is bounded by the parameters σ_i, ρ_i, and ν_i, which are related to the hardcore distance H_i. These constraints are functionally implemented through the path loss function $\ell(\cdot)$, which models the decay of signal strength with distance in wireless networks.

Since the MHCPP is a stationary point process, we can place the user of the i-th class at the origin without loss of generality and denote its dedicated transmitter by $x_0 \in \Phi_i$. In a network with M classes of users, the total interference received by the user at the origin can be expressed as:

$$I_i = \sum_{j=1}^{M} \sum_{x_k \in \Phi_j \setminus \{x_0\}} P_j h_{x_k} \ell(\|x_k\|). \tag{9}$$

If we consider the scenario without fading, i.e., $h_{x_k} = 1$, the interference received by the user in the i-th class can be bounded from above as:

$$I_i \leq \sum_{j=1}^{M} P_j A_{\ell_j} - P_i \ell(r_0). \tag{10}$$

For different target SINR thresholds $\theta_i > 0$ given to different classes of users, the link reliability of i-th class is:

$$P_{\mathrm{s}}(\theta_i \mid \Phi) \triangleq \mathbb{P}(\mathrm{SINR}_i > \theta_i \mid \Phi), \tag{11}$$

where $\Phi = \bigcup_{i=1}^{M} \{\Phi_i\}$ represents the superposition of the point processes corresponding to M classes of users, and $P_{\mathrm{s}}(\theta_i \mid \Phi) \in [0,1]$ is a random variable conditioned on the locations of the transmitters. Link reliability can be interpreted as the probability that the SINR of a link with its user located at the origin exceeds the threshold θ_i, given a network realization Φ, and accounting for the effects of fading. The distribution associated with $P_{\mathrm{s}}(\theta_i \mid \Phi)$ is known as the *meta distribution* [21], [22].

Although the link reliability $P_{\mathrm{s}}(\theta_i \mid \Phi)$ is subject to randomness due to fading, a definite lower bound x_i can be established for users in the i-th class such that

$$\mathbb{P}\left(P_{\mathrm{s}}\left(\theta_i \mid \Phi\right) > x_i\right) = 1. \tag{12}$$

This value, x_i, is termed the reliability lower bound for all links associated with the i-th class. Similarly, if we require that 80% of the links meet the SINR threshold requirement, it can be expressed as $\mathbb{P}\left(P_{\mathrm{s}}\left(\theta_i \mid \Phi\right) > x_i\right) = 0.8$.

The challenge then is to determine how to achieve a deterministic lower bound x_i for all links of the i-th class of users within a large-scale wireless network with multiple users of varying priorities, through our proposed regulatory measures.

B. Link Reliability

For users in the i-th class with a target SINR threshold $\theta_i > 0$, considering the scenario of Rayleigh fading channels, the link reliability given by Eq. (11) is:

$$\begin{aligned} P_{\mathrm{s}}(\theta_i \mid \Phi) &\overset{(\mathrm{a})}{=} \mathbb{P}\left[\frac{P_i h_x \ell(r_0)}{I+W} > \theta_i \middle| \Phi\right] \\ &\overset{(\mathrm{b})}{=} \mathbb{E}\left[\exp\left(-\frac{\theta_i(I+W)}{P_i \ell(r_0)}\right) \middle| \Phi\right], \end{aligned} \tag{13}$$

where (a) arises from the definition of SINR, (b) follows from the property that h_x, the small-scale fading factor, adheres to an exponential distribution, and P_i represents the power allocated to the i-th class of transmitters.

Considering the forms of interference, the link reliability for the i-th class user in a large-scale wireless network, which encompasses M classes of users, can be calculated by:

$$\begin{aligned} P_{\mathrm{s}}\left(\theta_i \mid \Phi\right) &= \exp\bigg(-\frac{\theta_i W}{P_i \ell(r_0)}\bigg) \\ &\times \mathbb{E}\bigg[\exp\bigg(-\frac{\theta_i\Big(\sum_{j=1}^{M}\sum_{x_k\in\Phi_j\setminus\{x_0\}} P_j h_{x_k}\ell(\|x_k\|)\Big)}{P_i\ell(r_0)}\bigg)\bigg]. \end{aligned} \tag{14}$$

where $x_0 \in \Phi_i$ denotes a dedicated transmitter for the i-th class of uses.

C. Bound of Link Reliability

By applying the principles of spatial network calculus, the upper bounds of the power and the lower bounds of the link reliability in a wireless network can be derived.

Consider a wireless network where the transmitters related to the i-th user class are distributed as a hardcore point process Φ_i on $\mathbb{R}^2$ with a minimum separation distance (hardcore distance) H_i. Therefore, the distribution of transmitters corresponding to all classes of users is a superposition of Φ_i, i.e., $\Phi = \bigcup_{i=1}^{M}\{\Phi_i\}$. This setup implies that the point process Φ_i is strongly $(1, 2\pi/(\sqrt{12}H_i), \pi/(\sqrt{12}H_i^2))$-ball regulated. For all $R > 0$, there is a theoretical upper limit on the total number of transmitters across all classes, expressed as:

$$N(R) \triangleq \sum_{i=1}^{M} N_i(R) \le \tilde{\sigma} + \tilde{\rho}R + \tilde{\nu}R^2, \tag{15}$$

where $\tilde{\sigma} = \sum_{i=1}^{M}\sigma_i$, $\tilde{\rho} = \sum_{i=1}^{M}\rho_i$ and $\tilde{\nu} = \sum_{i=1}^{M}\nu_i$.

Let Φ_i be a Matérn hardcore point process on $\mathbb{R}^2$, $b(o,r) \subset \mathbb{R}^2$ denote the circular area with $r > 0$ centered at the origin and $N_i(r) \triangleq \Phi_i(b(o,r))$ denote the number of transmitters for the i-th class of users in $b(o,r)$. Let the total power allocated to all transmitters in the entire wireless network be denoted as P_{total}, and consider that there are M classes of users, with their transmitters' location distributions corresponding to specific hardcore distance H_i. Thus, P_{total} can be calculated as:

$$\begin{aligned} P_{\mathrm{total}} &= \sum_{i=1}^{M} N_i(r)P_i \le \sum_{i=1}^{M}(\sigma_i + \rho_i r + \nu_i r^2)P_i \\ &= \sum_{i=1}^{M} P_i + \sum_{i=1}^{M}\frac{2\pi}{\sqrt{12}}\left(\frac{P_i}{H_i}\right)r + \sum_{i=1}^{M}\frac{\pi}{\sqrt{12}}\left(\frac{P_i}{H_i^2}\right)r^2, \end{aligned} \tag{16}$$

where $\sigma_i = 1, \rho_i = 2\pi/(\sqrt{12}H_i), \nu_i = \pi/(\sqrt{12}H_i^2)$. This inequality shows an upper bound to the total transmission power of the network.

IV. Power Allocation Strategy

In this section, we explore the impact of the β-power allocation strategy on network performance, specifically under the conditions of the strong multi-priority $(\sigma_i, \rho_i, \nu_i)$-shot-noise regulation introduced earlier. We will examine how this strategy influences the distribution and utilization of power across different classes of users within the network. Additionally, we aim to derive a lower bound on the link reliability for networks with multi-priority users, demonstrating how strategic power allocation can enhance overall network reliability.

Within the network, power allocation strategies are tailored to meet the requirements of different user classes, ensuring equal power distribution within the same class while varying power across different classes based on their SINR thresholds. Higher priority classes with more stringent quality of service requirements receive more power to meet their needs. This leads us to the following power control scheme.

Definition 3. *(β-power allocation). Let $\beta > 0$ be a constant. The power P allocated to a link with a target SINR threshold θ is*

$$P = \ln(1 + \beta\theta), \tag{17}$$

According to Definition 3, the power allocated to each class must meet the minimum requirement to satisfy its designated SINR threshold, θ_i. For the i-th class, the minimum required power is

$$P_i = \ln(1 + \beta\theta_i), \tag{18}$$

where θ_i represents the lowest SINR threshold necessary for the users in the i-th class to achieve satisfactory service quality. This is inspired by Shannon's theorem and assumes that an increase in the SINR threshold θ_i indicates an increase in user demand.

Thus, the minimum transmit power required for each transmitter can be calculated based on the diverse SINR thresholds assigned to different classes of users. This helps to ascertain which user classes are capable of being satisfied under the current network settings and power allocation strategy.

First, let us consider the scenario where all classes of users achieve their required service levels and the transmitters located within a circular area of radius r where the number of transmitters corresponding to the i-th class of users is $N_i(r)$. The total power consumption for all transmitters within the network is given by:

$$\begin{aligned} P_{\text{total}} &= \sum_{i=1}^{M} N_i(r) P_i \\ &\leq \sum_{i=1}^{M} (\sigma_i + \rho_i r + \nu_i r^2) \ln(1 + \beta\theta_i). \end{aligned} \tag{19}$$

We address the problem of determining whether a reliability lower bound exists for the SINR threshold θ_i such that the following theorem holds.

Theorem 1. *Considering Rayleigh fading, if the transmit power P_i for the i-th class is β-power allocated and the point process Φ_i is multi-priority $(\sigma_i, \rho_i, \nu_i)$-shot-noise regulated, then the link reliability $P_{\mathrm{s}}(\theta_i \mid \Phi)$ satisfies:*

$$\begin{aligned} P_{\mathrm{s}}(\theta_i \mid \Phi) \geq & \exp\left(-\frac{\theta_i W}{P_i \ell(r_0)}\right) \\ & \times \exp\bigg(-\sum_{j=1}^{M} A_{\tilde{\ell}_j} + \tilde{\ell}_i(r_0)\bigg), \mathbb{P}\text{-}a.s., \end{aligned} \tag{20}$$

where $A_{\tilde{\ell}_j}$ denotes adjusted interference from other classes, Φ is the superposition of Φ_i.

Proof. The reliability $P_{\mathrm{s}}(\theta_i \mid \Phi)$ can be evaluated by integrating over the interference and noise as follows:

$$\begin{aligned} P_{\mathrm{s}}(\theta_i \mid \Phi) &= \mathbb{E}\left[\exp\left(-\frac{\theta_i (I + W)}{P_i \ell(r_0)}\right) \middle| \Phi\right] \\ &= \exp\left(-\frac{\theta_i W}{P_i \ell(r_0)}\right) \mathbb{E}\left[\exp\left(-\frac{\theta_i I}{P_i \ell(r_0)}\right) \middle| \Phi_i\right] \\ &= \exp\left(-\frac{\theta_i W}{P_i \ell(r_0)}\right) \prod_{j=1}^{M} \prod_{x_k \in \Phi_j \setminus \{x_0\}} \frac{1}{1 + \frac{\theta_i P_j \ell(\|x_k\|)}{P_i \ell(r_0)}} \\ &= \exp\left(-\frac{\theta_i W}{P_i \ell(r_0)}\right) \\ & \quad \times \prod_{j=1}^{M} \exp\bigg(-\sum_{x_k \in \Phi_j \setminus \{x_0\}} \ln\bigg(1 + \frac{\theta_i P_j \ell(\|x_k\|)}{P_i \ell(r_0)}\bigg)\bigg), \end{aligned} \tag{21}$$

where $\tilde{\ell}_j(r) \triangleq \ln\left(1 + \frac{\theta_i P_j \ell(r)}{P_i \ell(r_0)}\right)$ is non-increasing, monotonic, and bounded. By combining the equation (8), we get an explicit formula for an a.s. the lower bound on $P_{\mathrm{s}}(\theta)$ in the special case of Rayleigh fading. This derivation shows that the SINR exceeds the threshold θ_i with a probability constrained by noise and interference, providing a lower bound on the link reliability for i-th class users by considering the combined effects of power allocation and interference regulation. □

The above theorem holds for general path loss $\ell(\cdot)$. Specially, for the case where $\ell(r) = \min\{1, r^{-\alpha}\}$, we get

$$\begin{aligned} A_{\tilde{\ell}_j} =& \sigma_j \ln\left(1 + \frac{\tilde{\theta}_j}{\ell(r_0)}\right) \\ &+ \frac{\alpha \rho_j \tilde{\theta}_j \ {}_2F_1\left(1 - \frac{1}{\alpha}, 1; 2 - \frac{1}{\alpha}; -\frac{\tilde{\theta}_j}{\ell(r_0)}\right)}{(\alpha - 1)\ell(r_0)} \\ &+ \frac{\alpha \nu_j \tilde{\theta}_j \ {}_2F_1\left(1 - \frac{2}{\alpha}, 1; 2 - \frac{2}{\alpha}; -\frac{\tilde{\theta}_j}{\ell(r_0)}\right)}{(\alpha - 2)\ell(r_0)}. \end{aligned} \tag{22}$$

where $\tilde{\theta}_j = P_j \theta_i / P_i$.

V. Numerical Results

In this section, we delve into the performance evaluation of a wireless network serving two distinct classes of users, categorized based on their SINR thresholds: high-priority and low-priority. We conduct simulations to assess the practical effectiveness of our theoretical models and to compare the simulated outcomes with the theoretically derived lower bounds of link reliability. The simulation environment is configured with transmitters arranged in a triangular lattice within a circular region of radius $r = 100$ meters, adhering to hardcore distances $H_1 = 1$ meter for high-priority users and $H_2 = 1$ meter for low-priority users. This configuration ensures that the distribution of transmitters corresponding to users of different priorities is mutually independent and unaffected by users of other priorities. However, the i-th class of users are still subject to interference from the transmitters corresponding to users of other classes. The point process governing the locations of the transmitters Φ_i is strongly regulated by a $(1, 2\pi/(\sqrt{12}H_i), \pi/(\sqrt{12}H_i^2))$-ball regulation model, which provides a basis for calculating theoretical lower bounds and conducting rigorous simulations. The simulation parameters include SINR thresholds θ_1 and θ_2 for high-priority and low-priority users, respectively, assuming $\theta_1 > \theta_2 > 0$. Additional parameters are set as follows: power factor $\beta = 1$, noise power $W = 0$ and a distance $r_0 = 1$ meter between users and their dedicated transmitters. The path loss function is defined as $\ell(r) = \min\{1, r^{-\alpha}\}$. In subsequent analyses, we set the pass loss exponent, denoted as α, to 4. We define the reference threshold as θ, setting θ_1 equal to θ and θ_2 to $\theta - 3\mathrm{dB}$.

Fig. 3 illustrates the variation in the lower bounds of link reliability for two classes of users as their SINR thresholds (θ_1 and θ_2) change. This figure includes both simulation results and theoretical calculations for high-priority users and low-priority users respectively. For users with the same priority, the vertical gap represents the differences in the link reliability lower bound between simulation results and theoretical calculations. This discrepancy primarily influenced by the point process modeling the locations of transmitters and the path loss function. The horizontal gap indicates the difference in SINR threshold required to achieve the desired link reliability. Notably, when the link reliability exceeds 0.8, the horizontal deviations between the simulation results and the theoretical lower bounds are less than $3\,\mathrm{dB}$ for high-priority users and

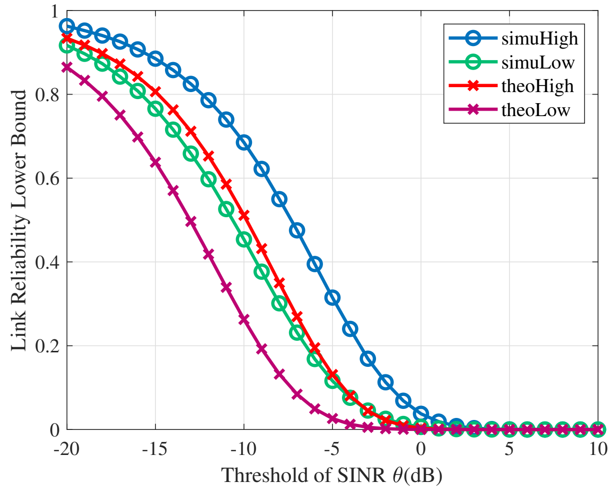

Fig. 3. Link Reliability vs. the Changes of the Users' Thresholds.

2 dB for low-priority users. As the SINR threshold increases, the lower bound of link reliability decreases. This indicates that higher user demands make it increasingly difficult to meet all user requirements. Low-priority users suffer from lower link reliability than high-priority users because their dedicated transmitters are allocated less power, leading to a lower SINR, thus necessitating a lower threshold to satisfy their requirements.

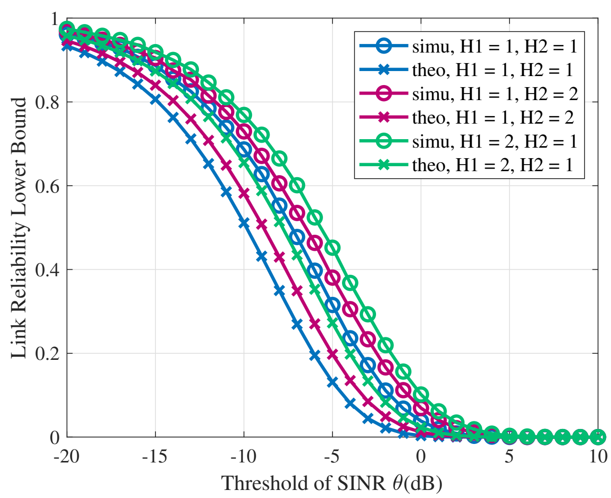

Fig. 4. Link Reliability with Different Hardcore Distances

Fig. 4 depicts the impact of different hardcore distances on the link reliability lower bound for high-priority users. This analysis considers scenarios where transmitters for high-priority and low-priority users are positioned at distinct hard-core distances. Specifically, when the hardcore distances H_1 and H_2 are both set to 1 meter, the link reliability lower bound reaches its minimum. This decrease is attributed to the increase density of transmitters, which intensifies the interference within the wireless network. Additionally, when the hardcore distances are set as $H_1 = 2$ meters and $H_2 = 1$ meter, a higher link reliability lower bound is observed. This improvement can be attributed not only to the reduced density of transmitters regulated by the hardcore distance, but also to the power allocation strategy, which allocates less power to low-priority transmitters, thereby reducing the overall level of interference within the wireless network.

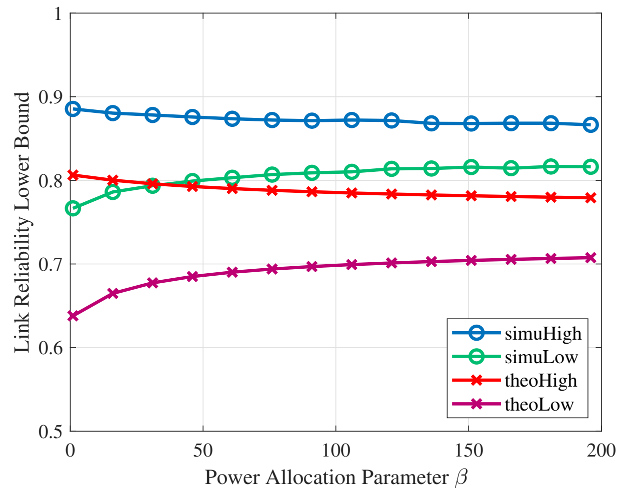

Fig. 5. Link Reliability vs. the Changes of β

In Fig. 5, the impact of the parameter β within the β-power allocation strategy on link reliability lower bound, with β varying from 1 to 200 and θ set at $-15\,\text{dB}$, is illustrated. It shows a clear increase in the link reliability lower bound for low-priority users as β increases, which coincides with a decrease in link reliability lower bound for high-priority users. Additionally, there is no optimal β value that achieves higher link reliability lower bound for both high-priority and low-priority users simultaneously.

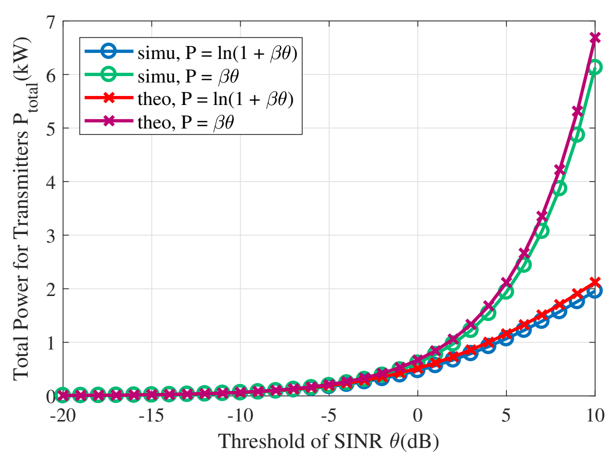

Fig. 6. Total Power for Transmitters vs. the Changes of θ

Fig. 6 examines the variations in total power consumption of the transmitters with changes in the SINR threshold θ,

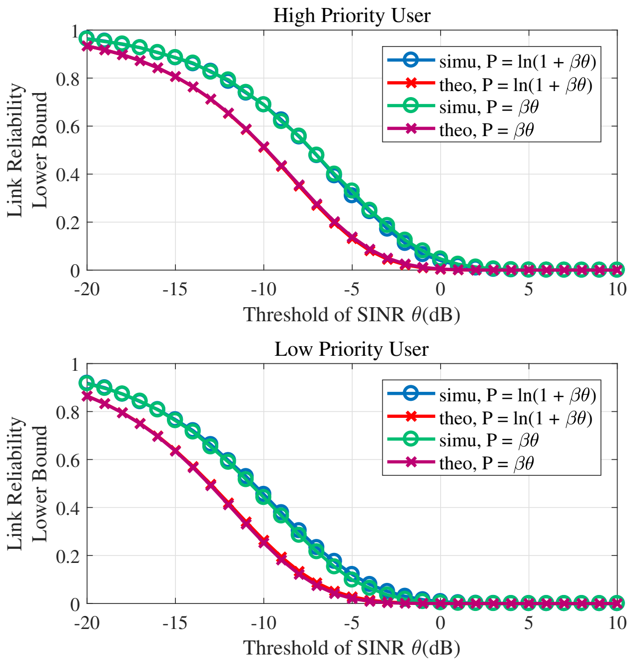

Fig. 7. Link Reliability Lower Bound vs. the Changes of θ

comparing two power allocation strategies: $P = \ln(1+\beta\theta)$ as mentioned in Def. 3 and $P = \beta\theta$. The theoretical results provide the upper bound on P_{total}, as derived from Eq. (16). The proposed power allocation strategy consumes less total power under every SINR thresholds, and the power difference continues to increase as the SINR threshold increases. This implies that utilizing the β-power allocation strategy is more effective to reduce power consumption. Fig. 7 presents a comparison of the link reliability lower bounds for high-priority and low-priority users under two different power allocation strategies, given equal total power for transmitters. The figures indicate that using the allocation strategy $P = \ln(1+\beta\theta)$ slightly enhances the link reliability lower bound for low-priority users, with no marked impact on high-priority users.

VI. Conclusion

This study introduced novel regulatory frameworks tailored for managing multi-priority traffic within large-scale wireless networks, utilizing the Matérn II method to ensure these regulations can be algorithmically implemented. Our work provides computable bounds on link performance suitable for various user priorities, establishing a robust analytical framework for evaluating network efficiency. Monte Carlo simulations validated our approach across different user classes, underscoring the practical relevance and efficacy of our regulatory strategies in real-world settings.

Looking ahead, our research will explore the integration of queuing theory in the time domain with spatial-temporal network calculus to enhance service quality across different priority levels. We also plan to assess the impacts of environmental factors such as shadowing and strategies such as dynamic power control and load balancing on network performance, aiming to refine and extend the performance guarantees essential for future wireless network deployments.

References

[1] Y. Hwang and S. Oh, "A study on ultra-reliable and low-latency communication technologies for 5G & 6G services," in *13th International Conference on Information and Communication Technology Convergence (ICTC)*. IEEE, 2022, pp. 1207–1209.

[2] Y. Zhong and X. Ge, "Toward 6G Carbon-Neutral Cellular Networks," *IEEE Network*, 2024, in press.

[3] C.-S. Choi, "Modeling and Analysis of Priority-Based Distributed Access Control in Vehicular Networks," *IEEE Trans. Veh. Technol.*, vol. 71, no. 6, pp. 6848–6852, 2022.

[4] N. Kumar, A. Ahmad, and D. K. Singh, "Priority Based Power Allocation in a Mobile Communication Network," in *IEEE International Conference on Power Energy, Environment and Intelligent Control (PEEIC)*, 2018, pp. 713–716.

[5] A. Abdel-Hadi and C. Clancy, "A utility proportional fairness approach for resource allocation in 4G-LTE," in *International Conference on Computing, Networking and Communications (ICNC)*. IEEE, 2014, pp. 1034–1040.

[6] J.-W. Lee, R. R. Mazumdar, and N. B. Shroff, "Opportunistic power scheduling for multi-server wireless systems with minimum performance constraints," in *IEEE INFOCOM*, vol. 2, 2004, pp. 1067–1077.

[7] Y. Zhong, G. Mao, X. Ge, and F.-C. Zheng, "Spatio-temporal modeling for massive and sporadic access," *IEEE Journal on Selected Areas in Communications*, vol. 39, no. 3, pp. 638–651, 2020.

[8] H. Q. Nguyen, F. Baccelli, and D. Kofman, "A stochastic geometry analysis of dense IEEE 802.11 networks," in *IEEE INFOCOM 2007-26th IEEE International Conference on Computer Communications*. IEEE, 2007, pp. 1199–1207.

[9] T. V. Nguyen, F. Baccelli, K. Zhu, S. Subramanian, and X. Wu, "A performance analysis of CSMA based broadcast protocol in VANETs," in *Proceedings IEEE INFOCOM*. IEEE, 2013, pp. 2805–2813.

[10] K. V. Mishra, B. S. MR, and B. Ottersten, "Stochastic-geometry-Based interference modeling in automotive radars using matern hard-core process," in *IEEE Radar Conference (RadarConf)*, 2020, pp. 1–5.

[11] M. Di Renzo, A. Zappone, T. T. Lam, and M. Debbah, "System-level modeling and optimization of the energy efficiency in cellular networksA stochastic geometry framework," *Trans. Wirel. Commun.*, vol. 17, no. 4, pp. 2539–2556, 2018.

[12] Z. Chen and Y. Zhong, "Characterizing Stability Regions in Wireless Networks With Hard-Core Spatial Constraints," *IEEE Wireless Communications Letters*, 2024, in press.

[13] J. Miao, Z. Hu, K. Yang, and et al., "Joint power and bandwidth allocation algorithm with QoS support in heterogeneous wireless networks," *IEEE Commun. Lett.*, vol. 16, no. 4, pp. 479–481, 2012.

[14] C. Liu, S. Zhang, X. Qin, and et al., "Utility-based resource allocation in OFDMA relay networks with service differentiation," in *IEEE Wireless Communications and Networking Conference (WCNC)*, 2011, pp. 72–77.

[15] C.-S. Chang, "Performance guarantees in communication networks," *Eur. Trans. Telecommun.*, vol. 12, no. 4, pp. 357–358, 2001.

[16] J.-Y. Le Boudec and P. Thiran, *Network calculus: a theory of deterministic queuing systems for the internet*. Springer, 2001.

[17] R. L. Cruz, "A calculus for network delay. I. Network elements in isolation," *IEEE Trans. Inf. Theory*, vol. 37, no. 1, pp. 114–131, 1991.

[18] K. Feng and F. Baccelli, "Spatial Network Calculus and Performance Guarantees in Wireless Networks," *IEEE Trans. Wirel. Commun.*, 2024.

[19] F. Baccelli, B. Błaszczyszyn *et al.*, "Stochastic geometry and wireless networks: Volume II applications," *Foundations and trends® in networking*, vol. 4, no. 1–2, pp. 1–312, 2010.

[20] M. Haenggi, R. K. Ganti *et al.*, "Interference in large wireless networks," *Foundations and Trends® in Networking*, vol. 3, no. 2, pp. 127–248, 2009.

[21] M. Haenggi, "The meta distribution of the SIR in Poisson bipolar and cellular networks," *Trans. Wirel. Commun.*, vol. 15, no. 4, pp. 2577–2589, 2015.

[22] K. Feng and M. Haenggi, "Separability, asymptotics, and applications of the SIR meta distribution in cellular networks," *IEEE Trans. Wirel. Commun.*, vol. 19, no. 7, pp. 4806–4816, 2020.